2006-01-3171

Residual Stress Prediction for Part Distortion Modeling

T. D. Marusich, S. Usui, S. Lankalapalli, N. Saini, L. Zamorano and A. Grevstad
Third Wave Systems

1.0 Problem Introduction

Residual stresses and part distortion are major obstacles to time-to-market, reduced scrap, and high part quality in metal machining. Aerospace monolithic structures suffer from distortions that hamper assembly operations. Automotive powertrain components have high flatness-tolerance surfaces that maintain fuel efficiency while lowering emissions. Problems persist because industry lacks a capability to predict machining induced residual stresses and part distortion.
One method of comprehensive distortion analysis is application of the finite element method (FEM). Here, a three-dimensional FEM model is presented that includes fully adaptive unstructured mesh generation, tight thermo-mechanical coupling, deformable tool-chip-workpiece contact, momentum effects at high speeds and constitutive models appropriate for high strain rate, and finite deformation analysis that predicts machining induced residual stresses. A complementary capability to translate the machining induced residual stress results and incorporate pre-existing stresses to a holistic part level analysis for part distortion prediction will be discussed.

2.0 Residual Stress Prediction with Finite Elements

Machining induced residual stress is predicted using *AdvantEdge*™, an explicit dynamic, thermo-mechanically coupled finite element model specialized for metal cutting. *AdvantEdge*™ uses a Lagrangian FEM approach with adaptive remeshing to resolve multiple length scales (i.e., cutting edge radius, secondary shear zone and chip load), multiple body deformable contact for tool-workpiece interaction, and transient thermal analysis. Workpiece material are represented with constitutive models that include effects of high strain rates, large strains, and short heating times that are present at the tool-chip interface in machining operations.

The finite deformation kinematic and stress update formulations can be found in Marusich and Ortiz [1]. They are reviewed here in brevity. The balance of linear momentum is written as

$$\sigma_{ij,j} + \rho b_i = \rho \ddot{u}_i$$

The weak form of the principal of virtual work becomes

$$\int_B v_i \sigma_{ij,j} + v_i \rho b_i dV = \int_B \rho v_i \ddot{u}_i dV$$

Integration by parts and rearranging terms provides

$$\int_B \rho v_i \ddot{u}_i dV + \int_B v_{i,j} \sigma_{ij} dV = \int_{\partial B} v_i \sigma_{ij} n_j d\Omega + \int_B v_i \rho b_i dV$$

which can be interpreted as
(Inertial Terms) + (Internal Forces)=(External Forces)+(Body Forces)

Finite element discretization provides

$$\int_B \rho N_a N_b \ddot{u}_{ib} dV + \int_B N_{a,j} \sigma_{ij} dV = \int_{\partial B} N_a \tau_i d\Omega + \int_B \rho N_a b_i dV$$

In matrix form

$$\mathbf{Ma}_{n+1} + \mathbf{R}^{int}_{n+1} = \mathbf{R}^{ext}_{n+1}$$

where

$$M_{ab} = \int_{B0} \rho_0 N_a N_b dV_o$$

is the mass matrix

$$R^{ext}_{ia} = \int_{B0} b_i N_a dV_o + \int_{\partial B0\tau} \tau_i N_a d\Omega_o$$

is the external force array and

$$R^{int}_{ia} = \int_{B0} P_{iJ} N_{a,J} dV_o$$

is the internal force array. In the above expressions, Na, a=1,…,numnp are the shape functions, repeated indices imply summation, and a comma (,) represents partial differentiation with respect to the corresponding spatial coordinate, and P_{iJ} is the first Piola-Kirchhoff stress tensor, analogous to the engineering or nominal stress.

Thermal Equations

Heat generation and transfer are handled via the second law of thermodynamics. A discretized weak form of the first law is given by

$$\mathbf{C}\dot{\mathbf{T}}_{n+1} + \mathbf{K}\mathbf{T}_{n+1} = \mathbf{Q}_{n+1}$$

A lumped capacitance matrix $\mathbf{C}$ is used to eliminate the need for any equation solving.

$$\mathbf{C}\dot{\mathbf{T}} + \mathbf{K}\mathbf{T} = \mathbf{Q}$$

where $\mathbf{T}$ is the array of nodal temperatures,

$$C_{ab} = \int_{Bt} c\rho\ N_a N_b dV_o$$

is the heat capacity matrix,

$$K_{ab} = \int_{B0} D_{ij} N_{a,i} N_{b,j} dV$$

is the conductivity matrix, and

$$Q_a = \int_{Bt} sN_a dV + \int_{B\tau q} hN_a dS$$

is the heat source array with h, having the appropriate value for the chip or tool.

In machining applications, the main sources of heat are plastic deformation in the bulk and frictional sliding at the tool-workpiece interface. The rate of heat supply due to the first is estimated as

$$s = \beta \dot{W}^{p}$$

where $\dot{W}^{p}$ is the plastic power per unit deformed volume and the Taylor-Quinney coefficient β is of the order of 0.9. The rate at which heat is generated at the frictional contact, on the other hand is

$$h = -\mathbf{t} \cdot \|\mathbf{v}\|$$

where $\mathbf{t}$ is the contact traction and $\|\mathbf{v}\|$ is the jump in velocity across the contact.

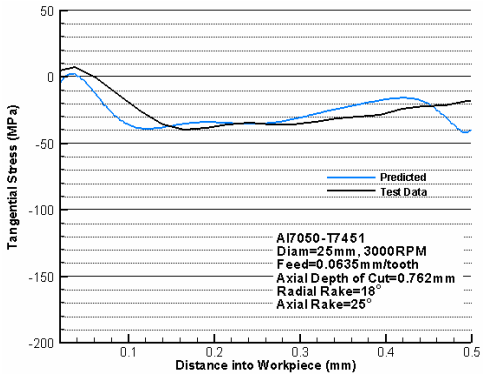

Figure 1. Tangential residual stress profile predicted by *AdvantEdge*™ compared with that measured by hole drilling in a face milling operation on Al7050.

To predict the residual stress imparted in the workpiece during a machining operation, an FEM simulation is designed by parametric specification of the cutting operation. This

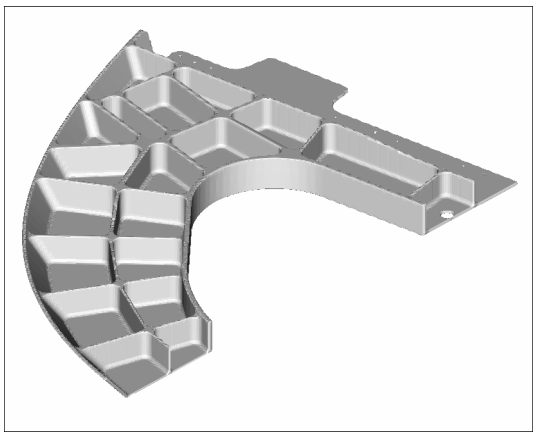

Figure 2. Initial solid model geometry of part used to demonstrate distortion prediction.

includes representation of the workpiece, Figure 2 and Figure 3, and tool materials, tool geometries, tool edge preparation, and machining in-feed, speed and depth of cut. Following simulation of the cutting process, the model is thermo-mechanically relaxed to provide an accurate representation of the residual stress state of the workpiece, Figure 4.

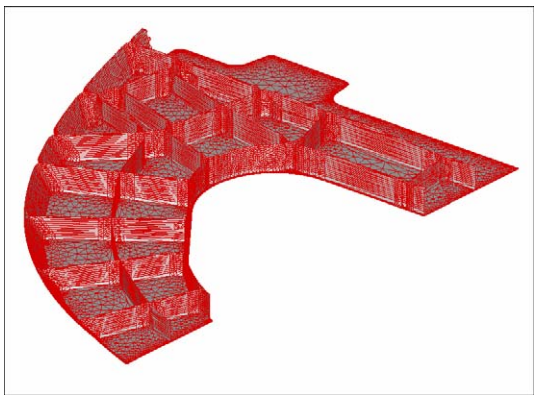

Figure 3. Mesh generated by Distortion Modeler.

3.0 Inputs in Distortion Analysis

AdvantEdge™ Distortion Modeler incorporates *AdvantEdge*™ FEM machining-induced residual stress prediction with bulk plate or forging residual stresses and clamping conditions to provide a prediction of final part distortion as a function of machining strategy (i.e., tool path variation, positioning of part in bulk plate, clamping strategies, and material selection). The workpiece representation contains bulk material stresses arising from forging, rolling or heat treatment. The machining process is modeled by taking into account the toolpath, speed and feed rates of the cutter. Machining induced stresses are applied as material is removed. The final part distortion is computed via an equilibrium calculation.

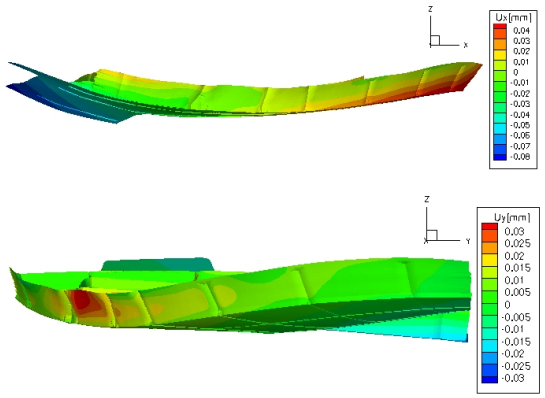

Figure 4. Distortion contours of part.

4.0 Results

The technique was provided to a thin-walled Al7050 airframe component of size approximately 1m by 1m. Three cases were analyzed – top, center, and bottom – each representing the position in the thickness of the starting plate material where the part was machined from. Tool path and clamping conditions where the same for each case. Maximum distortion magnitudes were recorded for each case, Figure 5.

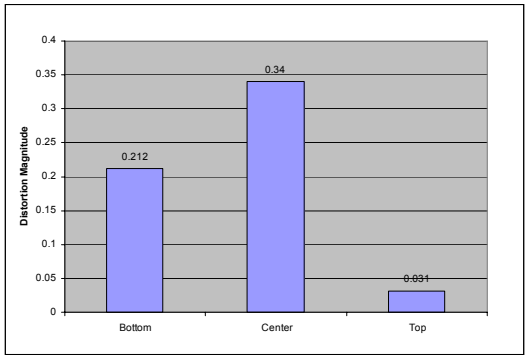

Figure 5. Maximum distortion magnitude as a function of machining position inside plate thickness. Part centered in thickness shows maximum distortion, part machined from top location shows minimum distortion.

5.0 Discussion

It can be seen that the maximum distortion magnitude can vary considerably depending on what position the part was machined from the plate, with the top position being most favorable (i.e., resulting in minimal distortion) in this case, Figure 5. It can be inferred that the bulk stresses existing in the initial plate as well as machining-induced stresses have significant effect on the final distortion configuration of the part. It is also seen that the distortion magnitude is highly dependent on part shape and symmetry.

6.0 Conclusion

A methodology is presented to model the distortion of a machined part caused by the existence of residual stresses. The combination of residual stresses from the bulk material, as well as those created by the machining process itself are considered. In this paper, the model is applied to an Al7050 component and the results are compared based on the position that the part was machined out of the initial plate stock. It is shown that distortion can be minimized based machining position in the plate.

7.0 References

1. Marusich, T. D. and Ortiz, M., "Modeling and Simulation of High-Speed Machining", Int. J. Num. Meth. Eng 38 (1995), 3675-94.